

# Motion-Dependent Representation of Space in Area MT+

Gerrit W. Maus,<sup>1,2,\*</sup> Jason Fischer,<sup>1,2,3</sup> and David Whitney<sup>1,2</sup>

<sup>1</sup>Department of Psychology, University of California Berkeley, Berkeley, CA 94720, USA

<sup>2</sup>Center for Mind and Brain, University of California Davis, Davis, CA 95618, USA

<sup>3</sup>Department of Brain and Cognitive Sciences and McGovern Institute for Brain Research, Massachusetts Institute of Technology, Cambridge, MA 02139, USA

\*Correspondence: [maus@berkeley.edu](mailto:maus@berkeley.edu)

<http://dx.doi.org/10.1016/j.neuron.2013.03.010>

## SUMMARY

How is visual space represented in cortical area MT+? At a relatively coarse scale, the organization of MT+ is debated; retinotopic, spatiotopic, or mixed representations have all been proposed. However, none of these representations entirely explain the perceptual localization of objects at a fine spatial scale—a scale relevant for tasks like navigating or manipulating objects. For example, perceived positions of objects are strongly modulated by visual motion; stationary flashes appear shifted in the direction of nearby motion. Does spatial coding in MT+ reflect these shifts in perceived position? We performed an fMRI experiment employing this “flash-drag” effect and found that flashes presented near motion produced patterns of activity similar to physically shifted flashes in the absence of motion. This reveals a motion-dependent change in the neural representation of object position in human MT+, a process that could help compensate for perceptual and motor delays in localizing objects in dynamic scenes.

## INTRODUCTION

One of the most well-studied cortical visual areas in primates is the middle temporal complex (area MT+). Despite a large and comprehensive body of literature, the way that MT+ represents visual space is debated. Area MT in the macaque monkey, and its human homolog hMT+, has been shown to represent positions coarsely in a retinotopic manner (Gattass and Gross, 1981; Huk et al., 2002; Wandell et al., 2007). Detailed mapping procedures revealed up to four retinotopic maps that collectively form the MT+ complex in humans (Dukelow et al., 2001; Amano et al., 2009; Kolster et al., 2010). Recently, some researchers have proposed that MT+ contributes to stable perception across eye movements by representing object locations in a world-centered, or spatiotopic, coordinate frame (Melcher and Morrone, 2003; d'Avossa et al., 2007; Ong et al., 2009; Crespi et al., 2011). Other researchers have found evidence for only ret-

inotopic, and not spatiotopic, coordinate frames in MT+ (Gardner et al., 2008; Morris et al., 2010; Hartmann et al., 2011; Ong and Bisley, 2011; Au et al., 2012; Golomb and Kanwisher, 2012), a difference that may be due to the location of covert visual attention (Gardner et al., 2008; Crespi et al., 2011). Most of these studies investigated spatial representations in MT+ at a relatively coarse spatial scale. However, during routine activities, such as navigating around obstacles or manipulating objects, the visual system's ability to localize objects on a fine spatial scale defines our ability to interact successfully with the world.

At a population level, MT+ represents fine-scale spatial information, discriminating position shifts of one-third of a degree of visual angle or less (Fischer et al., 2011). At these fine scales, a number of visual phenomena show remarkable dissociations between the perceived position of an object and its retinal or spatial position; for example, motion in the visual field can shift the perceived positions of stationary or moving objects (Fröhlich, 1923; Ramachandran and Anstis, 1990; De Valois and De Valois, 1991; Nijhawan, 1994; Whitney and Cavanagh, 2000; Krekelberg and Lappe, 2001; Whitney, 2002; Eagleman and Sejnowski, 2007). Disrupting activity in area MT+ by transcranial magnetic stimulation (TMS) reduces these motion-induced mislocalization illusions (McGraw et al., 2004; Whitney et al., 2007; Maus et al., 2013). This is strong evidence for an involvement of MT+ in these illusions, yet it does not resolve questions about the underlying spatial representation in area MT+. However, these findings raise the possibility that MT+ represents fine-scale positional biases induced by visual motion and that spatial representations in MT+ are dependent on visual motion.

Here, we investigated whether position representations in area MT+ are modulated by motion using the flash-drag effect (Whitney and Cavanagh, 2000; Tse et al., 2011; Kosovicheva et al., 2012). When flashes are presented in the vicinity of motion, they appear to be “dragged” in the direction of nearby motion and are perceived in illusory positions distinct from their physical (retinal) position (Figure 1). Our aim was to test whether position coding in MT+ reflects these perceptual distortions introduced by visual motion. We found that flashed objects presented near visual motion produced patterns of BOLD activity that were similar to patterns of activity generated by physically shifted flashes in the absence of motion. This reveals a motion-dependent change in the neural representation of object position in human MT+.

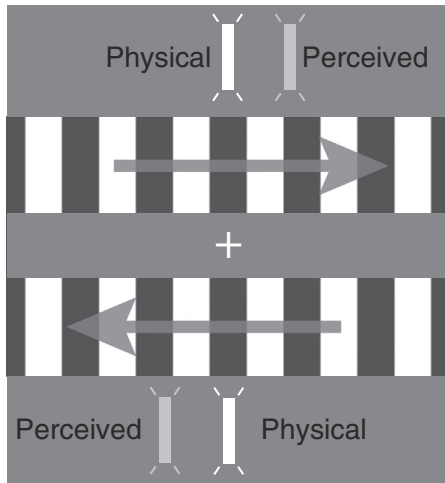


**Figure 1. The Flash-Drag Effect**

Visual motion can change the perceived position of brief flashes presented nearby; i.e., they appear “dragged” in the direction of motion.

**RESULTS**

**The Flash-Drag Effect**

First, we psychophysically quantified the magnitude of the perceptual shift in our flash-drag stimulus (Figure 2A). We presented a drifting grating in wedges along the horizontal and vertical visual field meridians, oscillating between inward and outward motion. In the spaces between the gratings, we presented flashed bars during either inward or outward motion (Figure 2B). There were three flashed bars in each visual field quadrant, scaled in size by their eccentricity (see Experimental Procedures). The flashes were presented in the same physical positions in all trials. After three presentations of the flashes, we presented comparison flashes whose positions were manipulated and shifted inward or outward by zero, one, or two bar widths on separate trials. Four participants performed a method of constant stimuli task, each participant judging whether the comparison flashes appeared shifted inward or outward relative to the flashes displayed while motion was present. Aggregate psychometric functions for this experiment are shown in Figure S1 (available online). Flashes presented during inward motion were perceived more centrally (closer to the fovea) than flashes presented during outward motion. In other words, flashes appeared to be shifted, or dragged, in the direction of the surrounding motion. The point of subjective equality (PSE) was shifted by 0.82 bar widths inward for flashes presented during inward motion and 0.16 bar widths outward for flashes during outward motion. Bootstrapped 95% confidence intervals of PSEs were not overlapping (horizontal error bars in Figure S1), and every individual observer showed a difference between PSEs in the expected direction.

Our stimuli were optimized for use in an fMRI experiment (i.e., flashes were presented repeatedly and distributed throughout the visual field to generate robust BOLD response). Participants were instructed not to attend to any one flash location specifically. For these reasons, we measured a relatively small flash-

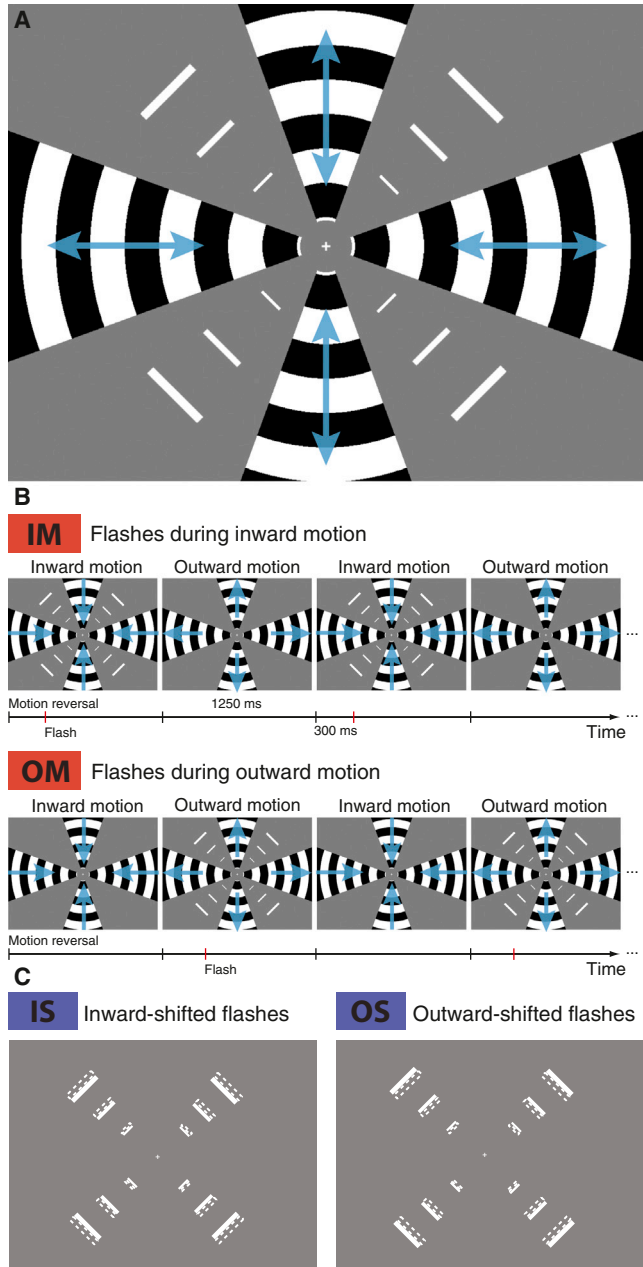


**Figure 2. Stimulus and Conditions in the fMRI Experiment**

(A) Gratings along the visual field meridians oscillated between inward and outward motion, and flashes were presented once per cycle in the space between the gratings.

(B) Both IM and OM conditions contained inward and outward motion, only the timing of the flashes relative to the phase of the oscillating motion changed.

(C) In IS and OS conditions, the physical position of flashes was shifted inward or outward by one bar width.

See also Figure S1.

drag effect in comparison to other studies (i.e., Whitney and Cavanagh, 2000; Tse et al., 2011; Kosovicheva et al., 2012), but the perceived shift of the flashes was robust and reliable. In the fMRI experiment, the observers’ perception of the flash-drag effect

was not explicitly probed; rather, subjects performed an attentionally demanding task at the fixation point to rule out possible attentional confounds. Our goal was to investigate whether visual motion leads to changes in the spatial representation of the flashes, regardless of the observer's task and attentional engagement.

### fMRI Experiment

The fMRI experiment consisted of six different stimulation conditions, presented in randomly interleaved blocks of 12 s duration: fixation only (F), motion only (M), flashes during inward motion (IM), flashes during outward motion (OM), physically inward-shifted flashes only (IS), and physically outward-shifted flashes only (OS) (see [Figures 2B](#) and [2C](#)). In the IM and OM conditions, the flashes were presented during either inward or outward motion, respectively, exactly once per oscillation cycle of the moving gratings. In each block, the motion was identical between both conditions, and the flashes were always presented in the same positions; only the timing of the flashes relative to the direction of motion was changed. In the IS and OS conditions, the position of each flash was shifted inward or outward (toward or away from the fovea, respectively) by the width of one flashed bar and, thus, roughly matched the perceptual mislocalization measured in the psychophysical study.

In all participants, we localized area MT+ in separate localizer runs by a contrast of moving and stationary random dot stimuli, as well as early visual areas V1–V3A, by a standard retinotopic mapping procedure (see [Experimental Procedures](#)). [Figure S2](#) shows the boundaries between retinotopic areas and the outline of MT+ on an “inflated” visualization of the cortical sheet for one participant. [Figure S2](#) also shows activity in response to the flashes alone (IS and OS) or the moving gratings alone (M). These maps were generated by fitting a general linear model (GLM) to the functional data and contrasting IS and OS versus F (baseline) and M versus F, respectively, with a false discovery rate threshold set at  $q = 0.05$ .

The flashes were centered in each visual field quadrant, and, accordingly, activity can be observed near the centers of quarterfield representations in areas V1–V3 ([Figure S2A](#)). Given that three flashes at different eccentricities were presented in each quadrant, we did not expect to see a clearly localized peak of BOLD activity at a single eccentricity in the retinotopic map. Instead, we pursued a sensitive multivoxel pattern analysis strategy that utilized information from a large number of voxels within a region of interest (ROI, see below).

The motion-only stimulus (M) consisted of four 40° wedges along the horizontal and vertical field meridians containing a high-contrast moving radial square-wave grating ([Figure 2A](#)). This stimulus generated robust activity throughout the visual cortex, which, not surprisingly, spread to portions of the cortical representation that did not correspond to stimulated locations ([Figure S2B](#)).

### Multivoxel Pattern Analysis

The conditions of main interest are IM and OM, where physically identical flashes were presented during either inward or outward motion of the gratings, respectively. Because we were interested in the representations of the flashes, and because the motion in

the IM and OM conditions was identical, we computed voxel-wise differences of GLM beta values between IM and OM conditions. This isolated the effect that the direction of motion in the grating wedges had on the representation of the flashes. Here, it is of crucial importance that stimulation in the moving wedges was identical between IM and OM conditions; the gratings always oscillated between inward and outward motion. Also, the flashes were always presented in the same physical position. Only the timing of the flashes relative to the motion differed between IM and OM conditions; i.e., they were presented during either inward or outward motion. The only activity remaining in these difference maps (IM-OM) reflects the influence of motion direction on the representation of the flashes.

Similarly, we computed the voxel-wise difference between GLM beta values for IS and OS (flashes physically shifted inward or outward, respectively). This resulted in a map (IS-OS) reflecting the differential representation of the physically shifted flashes.

We assessed the statistical similarity of the BOLD activity pattern evoked by illusory shifted flashes in the flash-drag effect to the BOLD activity evoked by physically shifted flashes. For this, we computed the correlation between the IM-OM difference map (flashes presented during inward minus outward motion) and the IS-OS map (inward- minus outward-shifted flashes). As mentioned above, IM and OM conditions consist of spatially identical visual stimulation; if MT+ represents object positions in a strictly retinotopic manner, then one would expect a difference map of these two conditions to only consist of noise. If, however, motion causes flashes to be represented similarly to physically shifted flashes in MT+, then we would expect a positive correlation between these two difference maps across a population of voxels; i.e., the physical shift of flashes between IS and OS conditions predicts how flashes are represented in the IM and OM conditions. Any reliably positive correlation is evidence for similarity in the representations of illusory shifted flashes and physically shifted flashes in the population of voxels.

[Figure 3](#) demonstrates this analysis in area MT+ for one participant. We selected an ROI of voxels representing the locations of the flashes by a GLM contrast of IS and OS versus F (flashes versus fixation;  $p < 0.01$ , Bonferroni corrected). We also repeated the analysis with independently defined ROIs and obtained the same results (see [Experimental Procedures](#)). [Figure 3A](#) shows the difference maps IM-OM and IS-OS, computed as described above, within this ROI. The difference values for each voxel are shown on a scatter plot in [Figure 3B](#). For the ROI in MT+ in this participant, which consisted of a total of 350 voxels, there is a positive correlation between the two difference maps ( $r = 0.729$ ), indicating similarity between the patterns of activity. Correlation coefficients  $r$  were transformed to Fisher  $z'$  scores to enable linear comparisons ( $z' = 0.928$ ).

To demonstrate that positive correlations are neither present everywhere in the brain nor an artifact of our analysis strategy, we conducted the following two analyses. First, we repeated the same correlation analysis for 1,000 sets of random voxels, picked (with replacement) from all cortical gray matter areas covered by our scan volume. Random sets of equal size (350 voxels) showed no correlation (mean  $z' = 0.000$ ,  $SD = 0.055$ ), and no single random set yielded higher correlations than

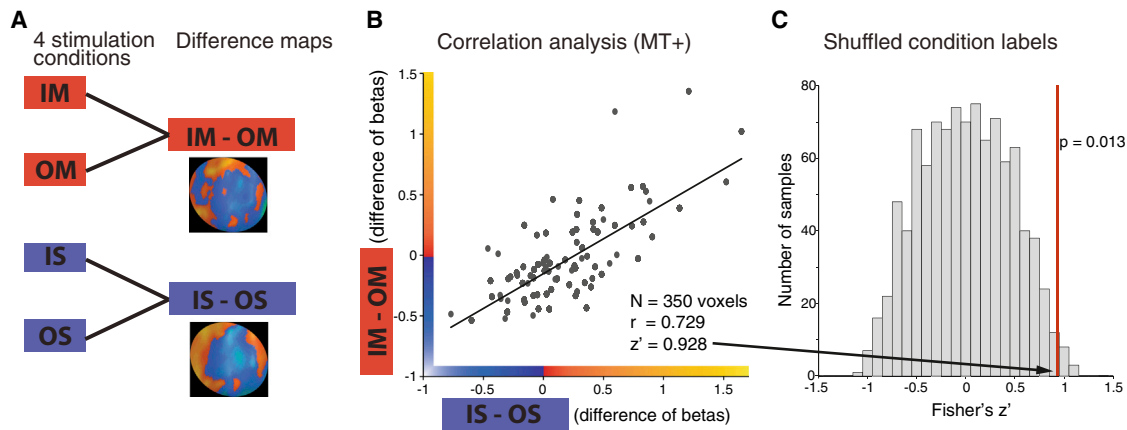


**Figure 3. Multivoxel Pattern Analysis Strategy**

(A) We calculated differences between flashes presented during inward and outward motion (IM-OM) and flashes in physical positions shifted inward and outward (IS-OS). Insets show maps for MT+ in one subject (the relevant color code can be found in [B]).

(B) These difference maps were correlated with each other for an ROI responding to the flashes within area MT+ (one subject shown; each point on the correlation plot is one voxel within MT+). A positive correlation signifies a similar representation of illusorily and physically shifted flashes.

(C) A histogram of resulting correlation values for the same voxels after random shuffling of condition labels.

See also Figure S2.

MT+ ( $p < 0.001$ ). Similar results were obtained for randomly selected contiguous gray matter regions from all brain areas. Notably, 1,000 randomly selected contiguous ROIs of the same size from all gray matter areas showed only small correlations (mean  $z' = 0.095$ ,  $SD = 0.011$ ); the mean correlation was significantly lower than that for the ROI in MT+ ( $p = 0.005$ ).

Furthermore, we assessed the significance of correlations using a permutation test. Using the same functional data, we randomly shuffled the condition labels of the IM and OM conditions 1,000 times. With the use of this reshuffling of IM and OM condition labels, the information about the motion direction at the time of the flashes is lost, whereas slow temporal correlations and information about the presence of motion in the stimulus are kept in place. Applying the same analysis (fitting a GLM, generating difference maps of IS-OS and IM-OM, and calculating the correlations as above) resulted in a null distribution of correlation coefficients centered around zero (Figure 3C). The correlation score obtained with the original condition labels (indicated by the red vertical line) falls in the positive extreme end of the distribution ( $p = 0.013$ ).

The mean Fisher  $z'$  value across subjects for correlations between IS-OS and IM-OM in MT+ was 0.370 ( $SD = 0.147$ ). We assessed significance at the group level by a bootstrap procedure that tested whether mean correlations in the group were higher than expected under the null hypothesis, comparing the actual correlations to those obtained from shuffling condition labels (see Experimental Procedures). The correlation in MT+ was highly significant ( $p = 0.005$ ), indicating that the representation of the flashes in MT+ is biased in the direction of the perceptual shift. Similarly high correlations were found in area V3A ( $z' = 0.385$ ,  $p = 0.050$ ), a midlevel motion-sensitive area that has been implicated in other motion-induced positions shifts (Maus et al., 2010). Earlier areas showed positive, but nonsignificant, correlations (V1,  $z' = 0.157$ ,  $p = 0.111$ ; V2,  $z' = 0.027$ ,  $p = 0.437$ ; V3,  $z' = 0.100$ ,  $p = 0.274$ ; see Figures 4 and S3). The pattern of results

across visual areas cannot be explained by different numbers of voxels (Pearson's  $r = -0.151$ ,  $p = 0.434$ ) or different signal-to-noise ratios ( $r = -0.208$ ,  $p = 0.279$ ).

In an additional control analysis, we tested whether spatial representations in MT+ were of sufficient resolution to pick up small position shifts. We employed a multivoxel pattern classification approach by using a support vector machine (SVM) to classify the activity patterns from single blocks as stemming from IS or OS stimulation conditions and, separately, for IM and OM conditions. Feature selection and training of the SVM was performed on a different subset of the data than the evaluation of classification performance and cross-validated 200 times for different sets of training and test data (see Experimental Procedures). This SVM approach classified IS and OS conditions accurately, on average, on 67.1% of blocks and IM and OM conditions on 57.5% of blocks. Statistical significance of classification performance was assessed by a permutation test performed by randomly shuffling block condition labels 1,200 times and repeating the same analysis on shuffled labels. Classification performance was significantly better than expected from this empirical null distribution for IS versus OS ( $p = 0.003$ ) and marginally better for IM versus OM ( $p = 0.061$ ). These additional results confirm that spatial representations in MT+ and our MRI recording sequence are of sufficient resolution to measure small, but reliable, spatial shifts.

### Attention

Throughout the fMRI experiment, participants performed an attentionally demanding detection task, responding with a key press to a brief contrast decrement of the fixation cross. We analyzed proportions of correctly detected contrast decrements and reaction times (RT) in each of the stimulation conditions to test for differences of attentional engagement between conditions. The fixation (F) and motion-only (M) conditions, as well as the IM and OM conditions, led to equivalent performance,

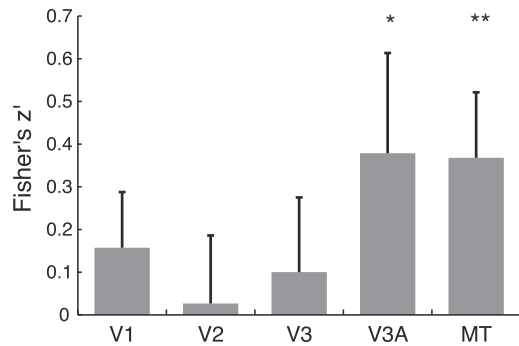


**Figure 4. Results of the Multivoxel Pattern Analysis**

Mean correlation scores ( $n = 6$ ) are shown for ROIs in V1–V3A and MT+. Error bars represent bootstrapped 95% confidence intervals.

See also Figure S3.

responses being between 87.7% and 89.3% correct and RT being between 0.53 and 0.57 s. Crucially, performance in the IM and OM conditions was no worse than in the baseline condition  $F$  (paired one-tailed  $t$  tests, RT,  $t[3] < -1.94$ ,  $p > 0.926$ ; accuracy,  $t[3] < 0.862$ ,  $p > 0.272$ ), ruling out attention to the positions of the flashes in the motion conditions as a cause for our effect. Performance was slightly (nonsignificantly) worse in the IS and OS conditions (76.8%–78.1% correct; paired two-tailed  $t$  tests,  $t[3] > 1.55$ ,  $p < 0.219$ ), and reaction times were longer (0.93–0.96 s;  $t[3] > 14.2$ ,  $p < 0.002$ ). However, attentional differences between motion conditions and flashes-only conditions would not affect our main analysis because we calculated differences in activation between IS and OS (and, separately, IM and OM) in order to assess correlations in patterns of activity. Performance and RTs between IS and OS (and between IM and OM) were equivalent (IS versus OS,  $t[3] < 2.58$ ,  $p > 0.082$ ; IM versus OM,  $t[3] < 0.613$ ,  $p > 0.584$ ).

## DISCUSSION

Here, we provide evidence that visual motion biases the fine-scale cortical localization of briefly presented objects in human MT+. The spatial coding of perceptually shifted objects (as a result of nearby motion) is similar to the coding of physically shifted objects in MT+. This representational change is small and would be hard to detect as a shift in the peak BOLD response within a retinotopic map with conventional analytic methods. Instead, we employed multiple flashes distributed throughout all four quadrants of the visual field and a sensitive analysis of multivoxel patterns. By calculating correlations between difference maps—the differences induced by a perceptual shift in the flash-drag effect and by physically different retinal positions—we were able to show that, in area MT+, the representation of stationary flashes in the flash-drag effect is biased in the direction of the motion.

The nature of spatial representations within area MT+ is debated. Some propose that MT+ represents positions in world-centered coordinates (Melcher and Morrone, 2003; d'Avossa et al., 2007; Ong et al., 2009; Crespi et al., 2011), others maintain that MT+ is strictly retinotopic (Gardner et al., 2008;

Hartmann et al., 2011; Au et al., 2012; Golomb and Kanwisher, 2012). Attention may be a key factor in determining which reference frame dominates in a given experiment (Gardner et al., 2008; Crespi et al., 2011). Our results go beyond these accounts, because flashes in identical physical locations (both in retinal and spatial coordinates) are represented differently in MT+ depending on the direction of visual motion present, and we ruled out that differences in attention can explain this effect (see below). Therefore, at a fine spatial scale—one that is critical for perception and action—MT+ incorporates information about visual motion in the scene into its position representation. An intriguing possibility is that spatial representations in MT+ are based on an integration of visual motion and other cues (such as retinal position and gaze direction). Consistent with this notion, a previous report has shown that patterns of fMRI activity in MT+ are highly selective for perceived object positions on a trial-by-trial basis (Fischer et al., 2011). Here, we systematically manipulated perceived positions of objects using a well-known motion-induced position illusion and demonstrated that position coding in MT+ is modulated by motion in a manner consistent with the perceived positions of the objects.

Our manipulation of perceived position was on a relatively fine spatial scale. Previous studies investigating spatial representations in MT+ have used large-scale manipulations of spatial positions; i.e., they were conducted with stimuli presented in either the left or right visual fields (d'Avossa et al., 2007; Golomb and Kanwisher, 2012). Here, we measure much more fine-grained spatial representations, which are, nonetheless, of the utmost importance for successful perception and action in dynamic environments. Localization errors of just fractions of a degree can mean the difference between, for example, successfully hitting or missing a baseball or avoiding a pedestrian while driving. At these fine spatial scales, localization errors due to neural delays of moving objects would have dramatic effects.

Motion-induced shifts in represented positions might improve the spatial accuracy of perception (Nijhawan, 1994, 2008) and visually guided behavior (Whitney et al., 2003; Whitney, 2008; Whitney et al., 2010) by compensating for neural delays in signal transmissions and coordinate transformations when localizing objects in dynamic scenes. Indeed, large-field visual motion, of the sort that MT+ is selective for, biases reaching movements in a manner that makes reaching more accurate (Whitney et al., 2003; Saijo et al., 2005); interfering with neural activity in MT+ with TMS reduces the beneficial effects of background visual motion on reaching (Whitney et al., 2007). More recently, Zimmermann et al. (2012) found that visual motion biases saccade targeting, which is consistent with the idea that background visual motion is used for predictively updating target positions for saccades, as well as for perception and visually guided reaching.

There are several neurophysiologically plausible mechanisms that could serve to shift the representation of objects in the direction of visual motion. For example, neurophysiological recordings in the visual cortices of monkeys (Sundberg et al., 2006) and cats (Fu et al., 2004) have shown that the spatial receptive field properties of neurons can change and shift in response to moving stimuli. Even in the retinae of salamanders and rabbits, receptive fields of ganglion cells are known to shift toward a

moving stimulus, effectively anticipating stimulation (Berry et al., 1999; Schwartz et al., 2007). These single-unit electrophysiological results were obtained with moving stimuli, and there are obvious differences between the BOLD signal and single unit recordings (i.e., Logothetis, 2003). However, the fMRI results in the present study point to similar motion-induced changes in population receptive fields in MT+ that affect spatial coding even for briefly presented static objects.

Previous single-unit studies in monkeys have found that MT+ receptive fields also shift with attention, even when no motion is present (Womelsdorf et al., 2006; Womelsdorf et al., 2008). However, attention cannot explain our pattern of results. The flash-drag effect is usually measured in psychophysical paradigms requiring observers to attend to the flash locations to be able to make perceptual judgments (Whitney and Cavanagh, 2000). In the present experiments, we presented observers with a stimulus that normally causes misperceptions of flash positions, but we did not require them to make perceptual judgments. Instead, observers performed an attentionally demanding task at the fixation point, and we analyzed the representation of passively viewed flashes in MT+. Performance for trials with inward- and outward-shifted flashes was equivalent to baseline trials, indicating no attentional capture of the flashes presented during motion. Thus, the representational change we found was not due to an effect of voluntary or involuntary attention to different spatial locations, nor did it require attention to be detectable in MT+.

The motion-dependent position coding in MT+ revealed here may play a causal role in perceiving object positions. With the use of TMS over area MT+, several studies have shown a reduction of motion-induced mislocalization phenomena during and after stimulation of MT+ (McGraw et al., 2004; Whitney et al., 2007; Maus et al., 2013). These studies show the causal necessity of activity in MT+ for perceptual localization. However, our present results go far beyond those studies. Previous TMS experiments could not address the spatial representation of objects in MT+, whether it is modulated by motion, whether MT+ causes changes in position representations in another area, or whether it actually represents shifted positions.

The present experiments provide evidence that motion-induced position shifts are represented by population activity in MT+. This provides insight into the way visual space is represented in area MT+ and how it contributes to visual localization of objects for perception and action.

## EXPERIMENTAL PROCEDURES

### Participants

Six participants (five males and one female; mean age 26.5 years old, range 22–29 years old), including two of the authors, volunteered to take part in the study. Four of the participants also took part in the psychophysical study outside of the scanner. All participants were informed about the procedure and thoroughly checked for counterindications for MRI, neurological health, and normal or corrected-to-normal visual acuity. The study was approved by the University of California Davis Institutional Review Board and performed in accordance with the Declaration of Helsinki.

### MRI Acquisition

The MRI scans were performed with a Siemens Trio 3T MR imaging device with an eight channel head coil at the UC Davis Imaging Research Center

(Sacramento, CA, USA). Each participant underwent a high-resolution T1-weighted anatomical scan with an MPRAGE sequence with  $1 \times 1 \times 1$  mm voxel resolution. Functional scans were obtained with a T2\*-weighted echo planar imaging sequence (repetition time = 2,000 ms, echo time = 26 ms, flip angle =  $76^\circ$ , matrix =  $104 \times 104$ ). The 28 slices (in plane resolution,  $2.1 \times 2.1$  mm; slice thickness, 2.8 mm; gap between slices, 0.28 mm) were oriented approximately parallel to the calcarine sulcus and covered all of the occipital and most of the parietal cortex but were missing inferior parts of the temporal and frontal cortices.

### Stimulus Presentation

In the psychophysics study, stimuli were presented on a cathode ray tube monitor (spatial resolution  $1024 \times 768$  pixels) running at a 75 Hz refresh rate. Participants viewed the screen from a 57 cm distance with their heads immobilized on a chin rest. In the MRI scanner, stimuli were back-projected onto a frosted screen at the foot end of the scanner bed with a Digital Projection Mercury 5000HD projector running at a 75 Hz refresh rate. Participants viewed the stimuli via a mirror mounted on the head coil. All stimuli were generated with MATLAB (MathWorks) and the Psychtoolbox extensions (Brainard, 1997; Pelli, 1997).

### Stimuli

The basic layout of the stimulus is shown in Figure 2A. The moving stimulus was a concentric square-wave grating (spatial frequency, 0.4 cycles per degree) that was visible only in wedges spanning an angle of  $40^\circ$  along the horizontal and vertical visual field meridians. White and black parts of the grating had a luminance of  $75.8 \text{ cdm}^{-2}$  and  $3.51 \text{ cdm}^{-2}$ , respectively (Michelson contrast = 91%). The grating's carrier wave drifted within the wedges at a constant speed of  $9.1^\circ/\text{s}$  (8 pixels per frame) and reversed direction every 1.25 s. The central area,  $1.8^\circ$  around the fixation cross, and the area between the grating wedges were uniform gray (luminance  $25.3 \text{ cdm}^{-2}$ ). White flashes could be presented in the areas between the gratings. To maximize BOLD response to the flashes, we presented several flashes (three in each sector of the visual field) scaled in size with eccentricity (see Figure 2A). The innermost flashes (at  $2.9^\circ$  eccentricity) measured  $0.9^\circ \times 0.1^\circ$ , the next flashes (at  $5.4^\circ$ ) measured  $1.7^\circ \times 0.2^\circ$ , and the outermost flashes (at  $7.9^\circ$ ) measured  $2.5^\circ \times 0.3^\circ$ . The flashes were presented 300 ms after a reversal of motion direction in the gratings and lasted two refresh frames (26.7 ms).

### Psychophysics Procedure and Analysis

To verify that our stimuli gave rise to the perception of the flash-drag effect, we performed a psychophysical study outside of the scanner. We presented three cycles of the grating wedges oscillating between inward and outward motion with flashes presented once per cycle during either inward or outward motion. Immediately afterward, the gratings remained stationary, and the flashes were presented one more time in physically altered locations. All flashed bars could be shifted inward or outward by one or two times their own width. Observers were asked to judge, without attending to any one flash location in particular, whether, on the final presentation, the flashes appeared spaced closer or wider (shifted inward or outward) than when presented during the motion. Four observers performed 100 trials in a method of constant stimuli design (2 motion directions during flashes [inward and outward]  $\times$  5 physical comparison flash positions [shifted by  $-2, -1, 0, 1,$  and  $2$  bar widths]  $\times$  10 repetitions).

To analyze this experiment, we fitted cumulative Gaussian functions to observers' responses, estimated PSEs where the flashes in physically shifted positions were perceived in the same positions as those presented during motion, and determined confidence intervals for these values (Wichmann and Hill, 2001a, 2001b).

### fMRI Procedure

In the fMRI experiment, there were six different stimulation conditions (F, M, IM, OM, IS, and OS). In the conditions with flashes during motion (IM and OM), the flashes were presented exactly once per oscillation cycle during either inward drift or outward drift, 300 ms after the reversal of motion direction in the gratings (Figure 2B). The phase of the grating's dark and light bars, and the phase of the motion direction oscillating between inward and outward at the start of each trial, was randomized. Overall, the motion was equated

between these two conditions; only the timing of the flashes relative to the direction of motion was changed. In the flashes-only conditions (IF and OF), the position of each flash was shifted inward or outward by the width of one bar (i.e., scaled by eccentricity; Figure 2C) from the original position in the IM and OM conditions. Flashes were repeated continuously at 4 Hz (i.e., flashed every 0.25 s).

In this experiment, we used a blocked design; i.e., each stimulus condition was shown continuously for 11.5 s (with a 0.5 s fixation-only period before the next stimulus condition started). Each subject completed a scan session containing six runs of the main experimental stimuli, which consisted of four repetitions of the F, M, IS, and OS conditions and seven repetitions of the IM and OM conditions. All stimulus conditions were presented in a randomly interleaved order. Each run started and ended with 4 s of fixation only. Throughout a run (i.e., during all conditions), participants performed an attentionally demanding task at the central fixation cross. The white fixation cross ( $0.3 \times 0.3^\circ$ ) decreased contrast randomly every 4–8 s (at least once during every stimulation block). Participants had to press a button on the response box as soon as they detected each contrast decrement. Due to technical difficulties with the response boxes, responses could not be recorded from one participant and could only be recorded in half of the runs from two more participants.

To define cortical areas, we performed independent localizer runs. To identify area MT+, we presented a stimulus consisting of low-contrast black and white random dots on a gray background that were either stationary for the duration of a block or oscillated between centrifugal and centripetal motion (speed of motion,  $7^\circ/\text{s}$ ; rate of oscillation, 1.25 Hz). To define the boundaries of retinotopic maps V1–V3A in the early visual cortex, we presented bow-tie-shaped flickering checkerboards along either the horizontal or vertical visual field meridian spanning a  $15^\circ$  opening angle and flickering at 4 Hz. These stimuli allowed us to identify the meridians separating early retinotopic areas in visual cortex.

### fMRI Analysis

The BrainVoyager QX software package (Brain Innovation) was used for the preprocessing and visualization of the data. Functional data from each run were corrected for slice acquisition time and head movements and spatially coregistered with each other. Voxel timecourses were temporally high-pass filtered with a cutoff at three cycles per run (0.008 Hz). We did not perform spatial smoothing. Then, functional data were aligned with the high-resolution anatomical scan, spatially normalized into Talairach space (Talairach and Tournoux, 1988), and subsampled into isotropic voxels of  $2 \times 2 \times 2$  mm. Furthermore, we separated white from gray matter and used the resulting boundary to “inflate” each brain hemisphere for better visualization of the cortical sheet. Spatial normalization was performed solely to facilitate the comparison of coordinates between subjects. All analysis was performed on single subjects, and there was no averaging of functional imaging data between subjects.

We analyzed localizer runs by fitting a GLM using BrainVoyager’s canonical hemodynamic response function. We corrected for serial correlations by removing first-order autocorrelations and refitting the GLM. For the delineation of areas V1–V3A, we contrasted stimulation conditions of horizontal versus vertical meridians and drew lines by hand along the maxima and minima of the unthresholded *t* map on the inflated representation of visual cortex. Area MT+ was defined by contrasting moving versus static dots.

All other analysis steps were performed with custom code in MATLAB. For the main experiment, we fitted a GLM to each voxel’s concatenated timecourse from all six runs using a boxcar model of the six stimulation conditions (F, M, IM, OM, IS, and OS) convolved with a canonical hemodynamic response function and corrected for serial autocorrelation. Beta values from the GLM were used as an index of a voxel’s activation in response to each stimulation condition. Then, we computed two difference maps, IM-OM and IS-OS (see Figure 3A). The stimulation caused by the moving wedges was identical in the IM and OM conditions, and flashes were always presented in identical positions. The only physical difference between the IM and OM conditions was in the timing of the flashes relative to the phase of the motion. The second difference map (IS-OS) represents the difference in activations resulting from the two physical flash positions. Similar to other multivoxel pattern analyses

(i.e., Haxby et al., 2001), we determined how similar a physical shift of the flashes is to the motion’s influence on the flash by correlating the values from the two difference maps IM-OM and IS-OS for a given set of voxels. The correlation approach is evaluating the similarity of the pattern of activity within an ROI rather than individual voxel’s activation values. Pearson’s correlation coefficients *r* were converted to Fisher *z*’ scores to facilitate linear comparisons of values.

We performed this correlation analysis for ROIs representing the positions of all flashes within area MT+ and early cortical maps (V1, V2, V3, and V3A). To define ROIs, we selected voxels with significant BOLD responses ( $p < 0.01$ , Bonferroni corrected) in response to the two flashes-only conditions (IS and OS). Signal-to-noise ratio within each ROI was assessed by calculating *t* values for the contrast of all stimulation conditions versus the fixation baseline. Notably, the selection of ROIs was orthogonal to the correlation analysis; the correlation used difference maps IM-OM and IS-OS, whereas the ROIs were defined by the union of IS and OS conditions, and these conditions were balanced in the experimental design (Kriegeskorte et al., 2009). However, to confirm that a selection bias did not influence our analysis, we also defined ROIs using independent data by splitting each subject’s functional data into odd and even runs, using one half of the data to select the ROIs and the other to perform the correlation analysis (and vice versa). The independently defined ROIs overlapped by 68.4% of voxels with ROIs based on the complete data set, and correlation scores did not statistically differ between ROIs defined on the basis of functional data from the same or different runs (paired *t* test,  $t(9) = 0.28$ ,  $p = 0.786$ ).

We verified that the observed correlations were specific to ROIs in the visual cortex by performing the same correlation analysis for randomly selected voxels and contiguous groups of voxels from all areas of the brain. We repeated the correlation analysis for 1,000 sets of random voxels of the same size as the original ROIs, picked (with replacement) from all cortical gray matter areas covered by our scan volume. We also selected 1,000 contiguous sets of voxels by growing spherical ROIs from randomly selected seed voxels within gray matter until the same number of voxels was reached. Correlation scores for these random sets of voxels formed null distributions to test the spatial specificity of the correlation effect between IM-OM and IS-OS difference maps.

To further assess the statistical significance of correlation scores, we employed a permutation test wherein we shuffled the condition labels of IM and OM conditions in each run 1,000 times, refitted the GLM, calculated the same difference maps, and performed the same correlation analysis as described above. The distribution of the resulting *z*’ scores represents the null hypothesis that there is no correlation between the difference maps, without making any assumptions about the underlying distribution. The proportion of shuffled samples leading to higher *z*’ scores to those obtained for the real, unshuffled labels represents a *p* value of committing a type I statistical error.

To assess statistical significance at the group level, we used the following approach. We wanted to assess whether the *z*’ score for a given area in each participant was reliably larger than it would be under the null hypothesis. For each participant, we randomly selected one of the shuffled sample *z*’ scores (above), subtracted it from the unshuffled *z*’ score, and calculated the mean of this difference across participants. Then, we repeated this procedure 1,000 times. The portion of the resulting distribution that is smaller than zero represents a *p* value for the hypothesis that the *z*’ score is larger than expected under the null hypothesis in the group.

An additional analysis used an SVM (Chang and Lin, 2011) to classify patterns of BOLD activity in area MT+ as stemming from either IS or OS conditions (and, separately, IM or OM conditions). Classification was performed on beta weights from a GLM that had one predictor for each block in the stimulus sequence from all six runs. In a feature selection step, a subset of voxels (~10%–15%) with maximal difference in mean activation between IS and OS (or IM and OM) was selected from the whole of MT+ for the classification procedure. This selection of voxels, and training of the SVM, was performed on a different subset of the timecourse data than the evaluation of classification performance and cross-validated 200 times for different randomly selected sets of training and test data. Statistical significance of classification performance was assessed by a permutation test, which randomly shuffled block condition labels 1,200 times and repeated the same analysis on shuffled labels.

### SUPPLEMENTAL INFORMATION

Supplemental Information contains three figures and can be found with this article online at <http://dx.doi.org/10.1016/j.neuron.2013.03.010>.

### ACKNOWLEDGMENTS

Parts of this work were presented at the European Conference on Visual Perception and the Annual Meeting of the Society for Neuroscience in 2009. The authors would like to thank E. Sheykhani and N. Wurnitsch for help with data collection and analysis. This research was supported by grant number EY018216 from the National Institutes of Health.

Accepted: March 3, 2013

Published: May 8, 2013

### REFERENCES

- Amano, K., Wandell, B.A., and Dumoulin, S.O. (2009). Visual field maps, population receptive field sizes, and visual field coverage in the human MT+ complex. *J. Neurophysiol.* *102*, 2704–2718.
- Au, R.K.C., Ono, F., and Watanabe, K. (2012). Time Dilation Induced by Object Motion is Based on Spatiotopic but not Retinotopic Positions. *Front Psychol* *3*, 58.
- Berry, M.J., 2nd, Brivanlou, I.H., Jordan, T.A., and Meister, M. (1999). Anticipation of moving stimuli by the retina. *Nature* *398*, 334–338.
- Brainard, D.H. (1997). The Psychophysics Toolbox. *Spat. Vis.* *10*, 433–436.
- Chang, C.-C., and Lin, C.-J. (2011). LIBSVM: a library for support vector machines. *ACM Transactions on Intelligent Systems and Technology* *2*, 1–27.
- Crespi, S., Biagi, L., d'Avossa, G., Burr, D.C., Tosetti, M., and Morrone, M.C. (2011). Spatiotopic coding of BOLD signal in human visual cortex depends on spatial attention. *PLoS ONE* *6*, e21661.
- d'Avossa, G., Tosetti, M., Crespi, S., Biagi, L., Burr, D.C., and Morrone, M.C. (2007). Spatiotopic selectivity of BOLD responses to visual motion in human area MT. *Nat. Neurosci.* *10*, 249–255.
- De Valois, R.L., and De Valois, K.K. (1991). Vernier acuity with stationary moving Gabors. *Vision Res.* *31*, 1619–1626.
- Dukelow, S.P., DeSouza, J.F., Culham, J.C., van den Berg, A.V., Menon, R.S., and Vilis, T. (2001). Distinguishing subregions of the human MT+ complex using visual fields and pursuit eye movements. *J. Neurophysiol.* *86*, 1991–2000.
- Eagleman, D.M., and Sejnowski, T.J. (2007). Motion signals bias localization judgments: a unified explanation for the flash-lag, flash-drag, flash-jump, and Frohlich illusions. *J. Vis.* *7*, 3.
- Fischer, J., Spotswood, N., and Whitney, D. (2011). The emergence of perceived position in the visual system. *J. Cogn. Neurosci.* *23*, 119–136.
- Fröhlich, F.W. (1923). Über die Messung der Empfindungszeit. *Zeitschrift für Sinnesphysiologie* *54*, 58–78.
- Fu, Y.X., Shen, Y., Gao, H., and Dan, Y. (2004). Asymmetry in visual cortical circuits underlying motion-induced perceptual mislocalization. *J. Neurosci.* *24*, 2165–2171.
- Gardner, J.L., Merriam, E.P., Movshon, J.A., and Heeger, D.J. (2008). Maps of visual space in human occipital cortex are retinotopic, not spatiotopic. *J. Neurosci.* *28*, 3988–3999.
- Gattass, R., and Gross, C.G. (1981). Visual topography of striate projection zone (MT) in posterior superior temporal sulcus of the macaque. *J. Neurophysiol.* *46*, 621–638.
- Golomb, J.D., and Kanwisher, N. (2012). Higher level visual cortex represents retinotopic, not spatiotopic, object location. *Cereb. Cortex* *22*, 2794–2810.
- Hartmann, T.S., Bremmer, F., Albright, T.D., and Krekelberg, B. (2011). Receptive field positions in area MT during slow eye movements. *J. Neurosci.* *31*, 10437–10444.
- Haxby, J.V., Gobbini, M.I., Furey, M.L., Ishai, A., Schouten, J.L., and Pietrini, P. (2001). Distributed and overlapping representations of faces and objects in ventral temporal cortex. *Science* *293*, 2425–2430.
- Huk, A.C., Dougherty, R.F., and Heeger, D.J. (2002). Retinotopy and functional subdivision of human areas MT and MST. *J. Neurosci.* *22*, 7195–7205.
- Kolster, H., Peeters, R., and Orban, G.A. (2010). The retinotopic organization of the human middle temporal area MT/V5 and its cortical neighbors. *J. Neurosci.* *30*, 9801–9820.
- Kosovicheva, A.A., Maus, G.W., Anstis, S., Cavanagh, P., Tse, P.U., and Whitney, D. (2012). The motion-induced shift in the perceived location of a grating also shifts its aftereffect. *J. Vis.* *12*, 1–14.
- Krekelberg, B., and Lappe, M. (2001). Neuronal latencies and the position of moving objects. *Trends Neurosci.* *24*, 335–339.
- Kriegeskorte, N., Simmons, W.K., Bellgowan, P.S.F., and Baker, C.I. (2009). Circular analysis in systems neuroscience: the dangers of double dipping. *Nat. Neurosci.* *12*, 535–540.
- Logothetis, N.K. (2003). The underpinnings of the BOLD functional magnetic resonance imaging signal. *J. Neurosci.* *23*, 3963–3971.
- Maus, G.W., Weigelt, S., Nijhawan, R., and Muckli, L. (2010). Does area V3A predict positions of moving objects? *Front Psychol* *1*, 186.
- Maus, G.W., Ward, J., Nijhawan, R., and Whitney, D. (2013). The perceived position of moving objects: transcranial magnetic stimulation of area MT+ reduces the flash-lag effect. *Cereb. Cortex* *23*, 241–247.
- McGraw, P.V., Walsh, V., and Barrett, B.T. (2004). Motion-sensitive neurones in V5/MT modulate perceived spatial position. *Curr. Biol.* *14*, 1090–1093.
- Melcher, D., and Morrone, M.C. (2003). Spatiotopic temporal integration of visual motion across saccadic eye movements. *Nat. Neurosci.* *6*, 877–881.
- Morris, A.P., Liu, C.C., Cropper, S.J., Forte, J.D., Krekelberg, B., and Mattingley, J.B. (2010). Summation of visual motion across eye movements reflects a nonspatial decision mechanism. *J. Neurosci.* *30*, 9821–9830.
- Nijhawan, R. (1994). Motion extrapolation in catching. *Nature* *370*, 256–257.
- Nijhawan, R. (2008). Visual prediction: psychophysics and neurophysiology of compensation for time delays. *Behav. Brain Sci.* *31*, 179–198, discussion 198–239.
- Ong, W.S., and Bisley, J.W. (2011). A lack of anticipatory remapping of retinotopic receptive fields in the middle temporal area. *J. Neurosci.* *31*, 10432–10436.
- Ong, W.S., Hooshvar, N., Zhang, M., and Bisley, J.W. (2009). Psychophysical evidence for spatiotopic processing in area MT in a short-term memory for motion task. *J. Neurophysiol.* *102*, 2435–2440.
- Pelli, D.G. (1997). The VideoToolbox software for visual psychophysics: transforming numbers into movies. *Spat. Vis.* *10*, 437–442.
- Ramachandran, V.S., and Anstis, S.M. (1990). Illusory displacement of equilluminous kinetic edges. *Perception* *19*, 611–616.
- Saijo, N., Murakami, I., Nishida, S.y., and Gomi, H. (2005). Large-field visual motion directly induces an involuntary rapid manual following response. *J. Neurosci.* *25*, 4941–4951.
- Schwartz, G., Taylor, S., Fisher, C., Harris, R., and Berry, M.J., 2nd. (2007). Synchronized firing among retinal ganglion cells signals motion reversal. *Neuron* *55*, 958–969.
- Sundberg, K.A., Fallah, M., and Reynolds, J.H. (2006). A motion-dependent distortion of retinotopy in area V4. *Neuron* *49*, 447–457.
- Talairach, J., and Tournoux, P. (1988). *Co-Planar Stereotaxic Atlas of the Human Brain* (Stuttgart: G. Thieme).
- Tse, P.U., Whitney, D., Anstis, S., and Cavanagh, P. (2011). Voluntary attention modulates motion-induced mislocalization. *J. Vis.* *11*, 12.
- Wandell, B.A., Dumoulin, S.O., and Brewer, A.A. (2007). Visual field maps in human cortex. *Neuron* *56*, 366–383.
- Whitney, D. (2002). The influence of visual motion on perceived position. *Trends Cogn. Sci.* *6*, 211–216.
- Whitney, D. (2008). Visuomotor extrapolation. *Behav. Brain Sci.* *31*, 220–221.

- Whitney, D., and Cavanagh, P. (2000). Motion distorts visual space: shifting the perceived position of remote stationary objects. *Nat. Neurosci.* 3, 954–959.
- Whitney, D., Westwood, D.A., and Goodale, M.A. (2003). The influence of visual motion on fast reaching movements to a stationary object. *Nature* 423, 869–873.
- Whitney, D., Ellison, A., Rice, N.J., Arnold, D., Goodale, M., Walsh, V., and Milner, D. (2007). Visually guided reaching depends on motion area MT+. *Cereb. Cortex* 17, 2644–2649.
- Whitney, D., Murakami, I., and Gomi, H. (2010). The utility of visual motion for goal-directed reaching. In *Space and Time in Perception and Action*, R. Nijhawan and B. Khurana, eds. (Cambridge: Cambridge University Press), pp. 121–145.
- Wichmann, F.A., and Hill, N.J. (2001a). The psychometric function: I. Fitting, sampling, and goodness of fit. *Percept. Psychophys.* 63, 1293–1313.
- Wichmann, F.A., and Hill, N.J. (2001b). The psychometric function: II. Bootstrap-based confidence intervals and sampling. *Percept. Psychophys.* 63, 1314–1329.
- Womelsdorf, T., Anton-Erxleben, K., Pieper, F., and Treue, S. (2006). Dynamic shifts of visual receptive fields in cortical area MT by spatial attention. *Nat. Neurosci.* 9, 1156–1160.
- Womelsdorf, T., Anton-Erxleben, K., and Treue, S. (2008). Receptive field shift and shrinkage in macaque middle temporal area through attentional gain modulation. *J. Neurosci.* 28, 8934–8944.
- Zimmermann, E., Morrone, M.C., and Burr, D. (2012). Visual motion distorts visual and motor space. *J. Vis.* 12, 1–8.

## Motion-Dependent Representation of Space in Area MT+

Gerrit W. Maus, Jason Fischer, and David Whitney

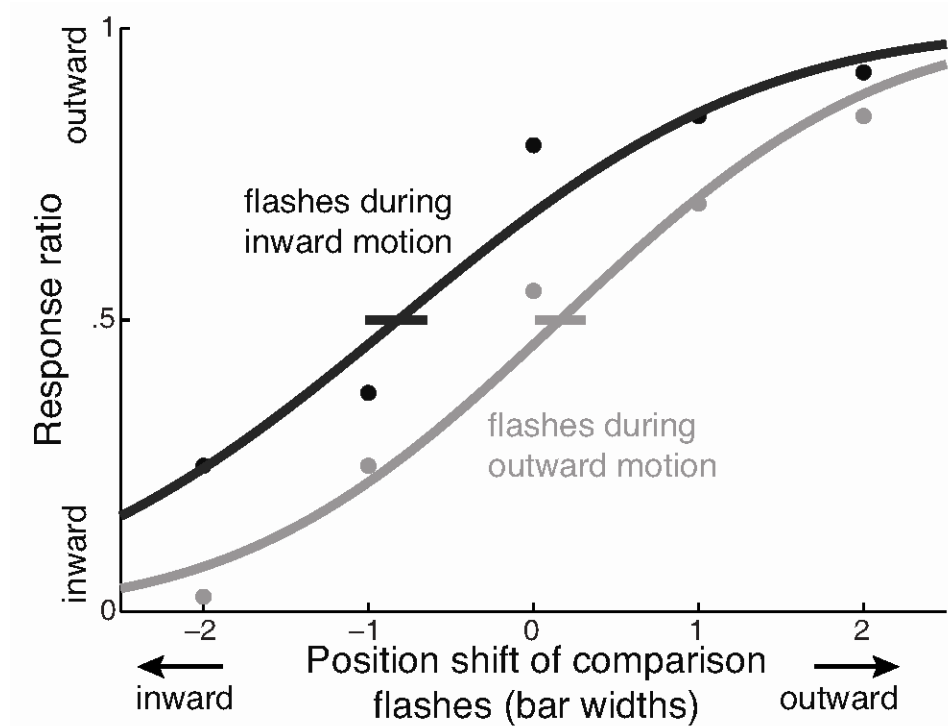


Figure S1. Psychophysical Results, Related to Figure 2

Results from the psychophysical experiment outside of the scanner. Flashes presented during inward motion (black) were perceived as shifted inward, and flashes during outward motion (grey) as shifted outward. Comparison flashes (without motion present) had to be shifted in the same direction as the motion to be perceived in the same position as the flashes during motion. Horizontal lines are bootstrapped 95%-confidence intervals around the point of subjective equality ( $n = 4$ ).

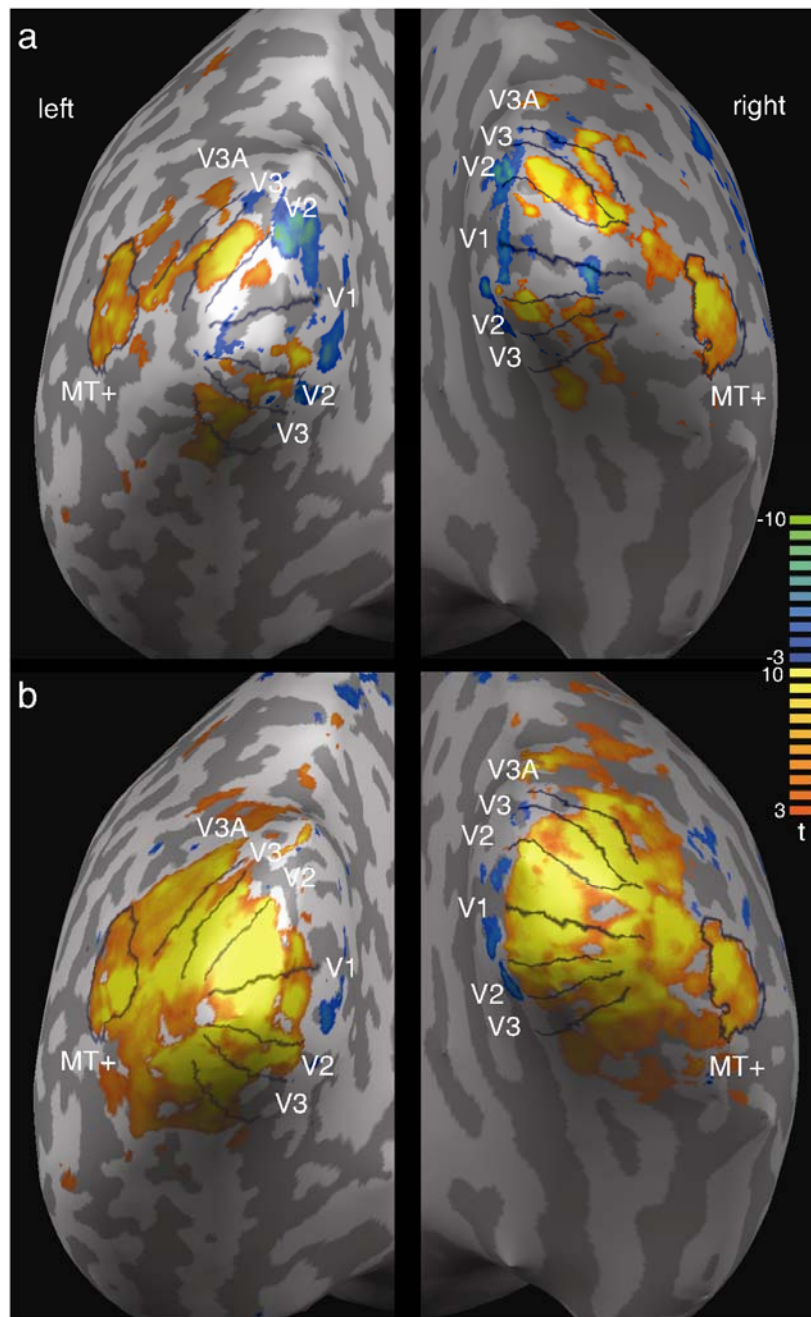


Figure S2. BOLD Responses in the Visual Cortex, Related to Figure 3

The view shows the inflated hemispheres, centered on the occipital poles for one participant. Lines depict the boundaries between early visual areas. The activity maps show BOLD activity (color-coded  $t$  values) in response to (a) flashes only (IS and OS conditions combined) and (b) motion only (condition M); False Discovery Rate threshold  $q = 0.05$ .

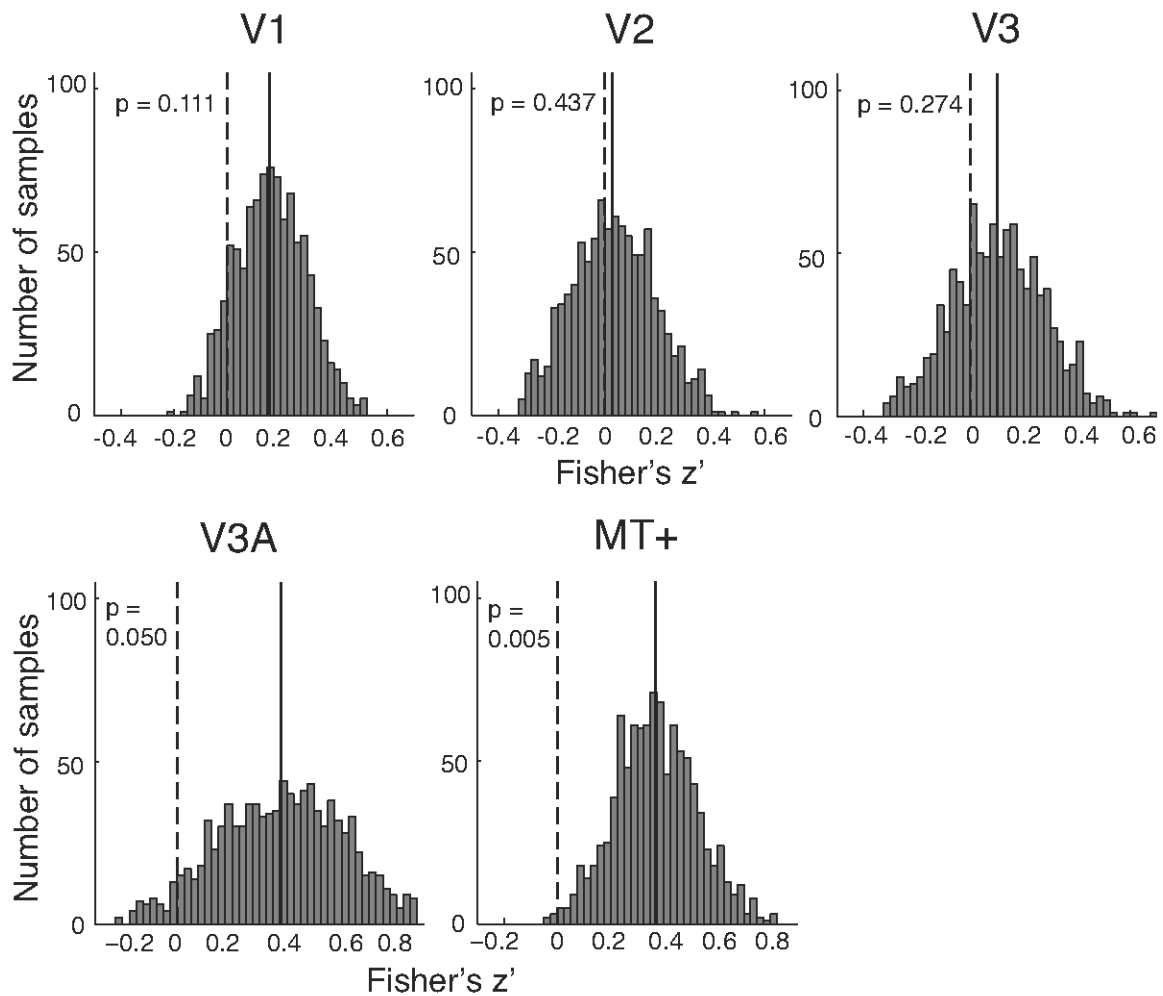


Figure S3. Results of Group Analysis, Related to Figure 4

Histograms show the group mean differences of correlation scores from correlations based on shuffled condition labels. We assessed whether the correlation  $z'$  score for a given area in each participant is reliably larger than it would be under the null hypothesis by randomly selecting one of the shuffled sample  $z'$  scores (Figure 3C), subtracting it from the unshuffled  $z'$  score, then calculating the mean of this difference across participants, and repeating this procedure 1000 times. The resulting distribution's portion that is smaller than zero represents a p value for the hypothesis that the  $z'$  score is larger than expected under the null hypothesis in the group. Dashed vertical lines show the null hypothesis ( $z' = 0$ ), solid lines the actual mean correlation scores (from Figure 4).